Doubly Cavitand-Capped Zn-Porphyrin Capsule with Simultaneous Encapsulation of Guest and Ligand, and Its Application to Doubly Cavitand-Capped Double-Decker Zn-Porphyrin Capsule

RESEARCH ARTICLE

Doubly Cavitand-Capped Zn-Porphyrin Capsule with Simultaneous Encapsulation of Guest and Ligand, and Its Application to Doubly Cavitand-Capped Double-Decker Zn-Porphyrin Capsule

Kakeru Nakabayashi,[a] Kazuki Kishimoto,[b] and Kenji Kobayashi*[a,b,c]

[a] K. Nakabayashi, Prof. Dr. K. Kobayashi
Department of Optoelectronics and Nanostructure Science, Graduate School of Science and Technology
Shizuoka University
836 Ohya, Suruga-ku, Shizuoka 422-8529 (Japan)
E-mail: kobayashi.kenji.a@shizuoka.ac.jp
[b] K. Kishimoto, Prof. Dr. K. Kobayashi
Department of Chemistry, Faculty of Science
Shizuoka University
836 Ohya, Suruga-ku, Shizuoka 422-8529 (Japan)
[c] Prof. Dr. K. Kobayashi
Research Institute of Green Science and Technology
Shizuoka University
836 Ohya, Suruga-ku, Shizuoka 422-8529 (Japan)

Supporting information for this article is given via a link at the end of the document.

Abstract: A 1:2 mixture of Zn-*meso*-tetrakis(4-dodecyl-3,5-dihydroxyphenyl)porphyrin (**1-Zn**) and tetrakis(4-pyridylethynyl)cavitand (**2**) in C_6D_6 self-assembles quantitatively into the doubly cavitand-capped Zn-porphyrin capsule **2•1-Zn•2** with two cavities divided by the porphyrin ring via eight ArOH···Npy hydrogen bonds. Simultaneous encapsulation of 1-acetoxy-3,5-dimethoxybenzene (**G**) and 4-(4-methylphenyl)pyridine (**L2**) in **2•1-Zn•2** preferentially occurs to form **G**/**L2**@(**2•1-Zn•2**). A 1:1 mixture of **1-Zn** and **2** in the presence of **G** and **L2** self-assembles into the **G**-encapsulating half-capsule **G**@(**2•1-Zn**)•**L2** with coordination of **L2** at the outer side of **2•1-Zn**. A 2:2:1 mixture of **1-Zn**, **2**, and 1,4-diazabicyclo[2.2.2]octane (**L3**) in the presence of **G** self-assembles preferentially into the **G**-encapsulating doubly cavitand-capped double-decker Zn-porphyrin capsule **G**/**G**@(**2•1-Zn•L3•1-Zn•2**) with coordination of **L3** between two hydrogen-bonded **1-Zn** subunits. Thus, selective formation of these cavitand–porphyrin capsules can be controlled by the stoichiometry of **1-Zn** and **2** as well as the character of N-ligands.

Introduction

Porphyrin derivatives possess particular electronic, photophysical, and catalytic properties. Therefore, porphyrin derivatives have been widely used as subunits for functional supramolecular architectures.[1] Supramolecular capsules are formed by self-assembly of preorganized modular subunits via intermolecular interactions to give an isolated nanospace.[2] Encapsulation of guest molecules in the capsules can provide various applications, such as separation techniques, stabilization of reactive intermediates, and sensing techniques by molecular recognition and capture.[2] Although self-assembled porphyrin capsules have been studied extensively,[3] porphyrin subunits have been used mainly as exterior panels of self-assembled capsules, and macrocyclic host-capped porphyrin capsules self-assembled by intermolecular interactions have been scarcely reported.[4,5] Recently, we reported that a 1:2 mixture of *meso*-tetrakis(4-dodecyl-3,5-dihydroxyphenyl)porphyrin (**1**)[6a] and a bowl-shaped tetrakis(4-pyridylethynyl)cavitand (**2**)[7] self-assembles into a doubly cavitand-capped porphyrin capsule **2•1•2** via eight ArOH···Npy hydrogen bonds (Figure 1).[6a] Capsule **2•1•2** possesses two cavities divided by the porphyrin ring and encapsulates two molecules of 1-acetoxy-3,5-dimethoxybenzene (**G**) as a guest to form **G**/**G**@(**2•1•2**).[6a] Zn-porphyrin provides a ligand-coordination site as a molecular recognition site.[5a,b] Therefore, Zn-porphyrin expands its potential as a building block for functional supramolecular architectures.[1,3] However, it is well known that the hydrogen bond between phenol and pyridine[8] is much weaker than the coordination bond between Zn-porphyrin and pyridine.[9,10] Our attention has focused on whether a 1:2 mixture of *meso*-tetrakis(4-dodecyl-3,5-dihydroxyphenyl)porphyrinato Zn(II) (**1-Zn**) and **2** (Figure 1) self-assembles into a thermodynamically stable doubly cavitand-capped porphyrin capsule **2•1-Zn•2**. Here, we report the quantitative formation of a self-assembled capsule **2•1-Zn•2** via eight ArOH···Npy hydrogen bonds without coordination bonds between **1-Zn** and **2** and its simultaneous encapsulation of two different guest molecules, namely, guest **G** and 4-(4-methylphenyl)pyridine (**L2**), to form **G**/**L2**@(**2•1-Zn•2**) (Scheme 1A). We also describe that a 2:2:1 mixture of **1-Zn**, **2**, and 1,4-diazabicyclo[2.2.2]octane (DABCO, **L3**) in the presence of **G** self-assembles preferentially into the **G**-encapsulating doubly cavitand-capped double-decker Zn-porphyrin capsule **G**/**G**@(**2•1-Zn•L3•1-Zn•2**) with coordination of **L3** between two hydrogen-bonded **1-Zn** subunits (Scheme 1B).

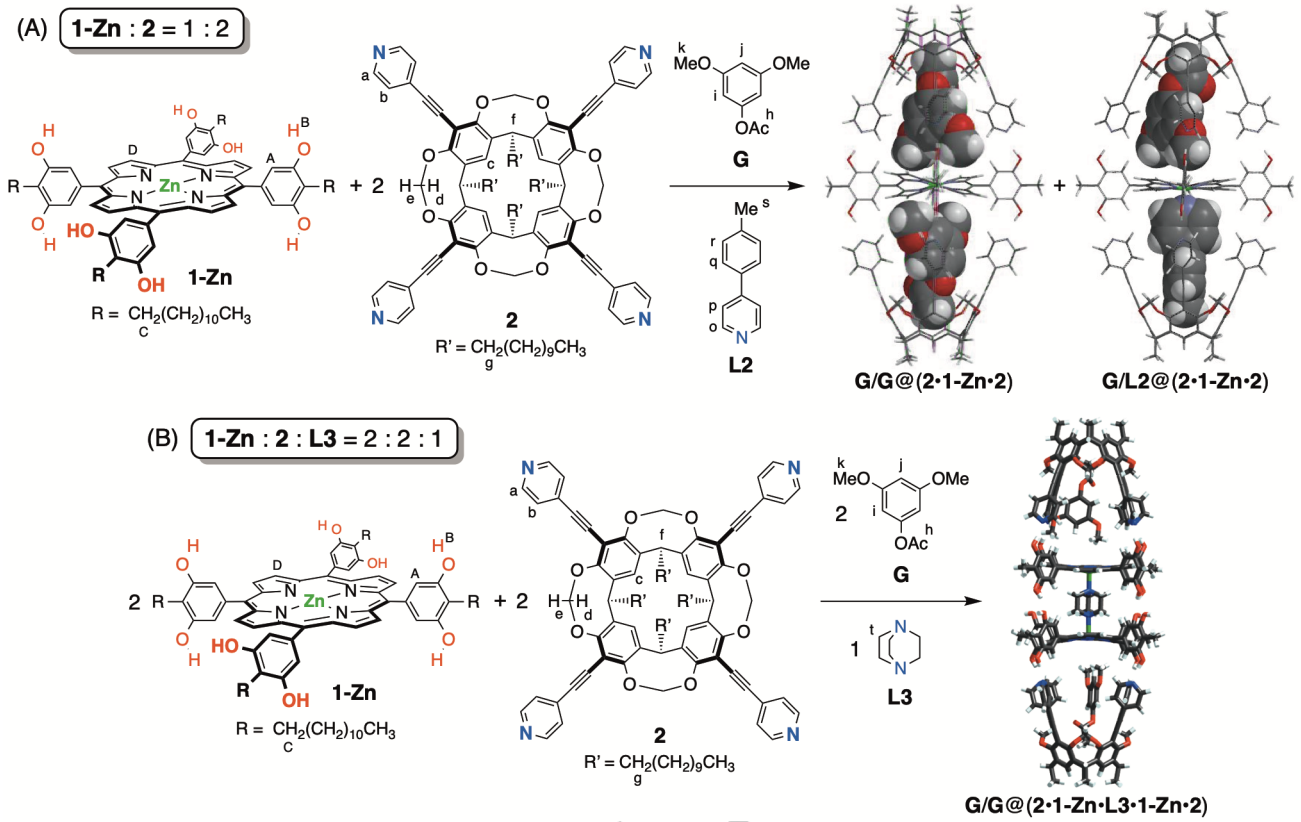

Scheme 1. (A) Self-assembly of a 1:2 mixture of **1-Zn** and **2** in the presence of **G** and **L2** into **G**/**G**@(**2**•**1-Zn**•**2**) and **G**/**L2**@(**2**•**1-Zn**•**2**). (B) Self-assembly of a 2:2:1 mixture of **1-Zn**, **2**, and **L3** in the presence of **G** into **G**/**G**@(**2**•**1-Zn**•**L3**•**1-Zn**•**2**). Molecular models are calculated at the PM3 level, wherein the dodecyl side chains of the subunit-**1-Zn** and the undecyl side chains of the subunit-**2** are replaced by methyl groups.

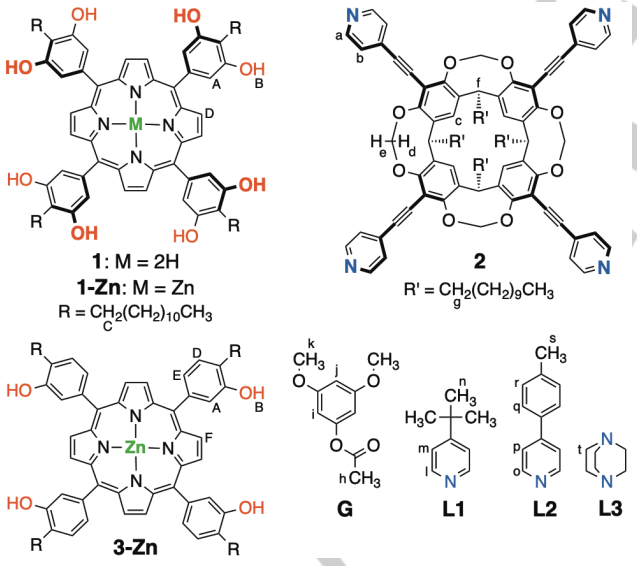

Figure 1. Structures of porphyrins **1**, **1-Zn**, and **3-Zn**, cavitand **2**, guest **G**, and N-ligands **L1**, **L2**, and **L3**.

Results and Discussion

Doubly Cavitand-Capped Porphyrin Capsule 2•1-Zn•2

Zn-porphyrin **1-Zn** alone is not soluble in C_6D_6. However, a 1:2 mixture of **1-Zn** and **2** becomes soluble in C_6D_6 after heating the mixture at 70 °C for 12 h. Hereafter, this heating condition is prerequisite for the complete dissolution and reaching equilibrium of molecular self-assembly containing **1-Zn**. The ^{1}H NMR spectrum of the mixture in C_6D_6 shows a highly symmetrical single species (Figure 2b), wherein the signals of the Pyα- and Pyβ-protons and the outer and inner protons of the methylene-bridge rim (O–$CH_{in}H_{out}$–O) of the cavitand subunit-**2** were shifted upfield by 0.56, 0.66, 0.35, and 0.43 ppm, respectively, relative to those of free **2** (Figure 2b vs. 2a), owing to the ring-current effect of the porphyrin subunit-**1-Zn**. Furthermore, the OH signal of the subunit-**1-Zn** in this species appeared at 11.34 ppm, which was shifted downfield by 7.01 ppm relative to that of soluble *meso*-tetrakis(4-dodecyl-3-hydroxyphenyl)porphyrinato Zn(II) (**3-Zn**, Figure 1)[6b] in C_6D_6. These chemical shift change values were almost the same as those of capsule **2•1•2** (Table S1 in the Supporting Information).[6a] These results clearly indicate the quantitative formation of the doubly cavitand-capped porphyrin capsule **2•1-Zn•2** via eight ArOH···Npy hydrogen bonds (Scheme 2), in a manner similar to **2•1•2**.[6a] The ^{1}H NMR signals of the ArH (δ = 7.71 ppm), the OH group (δ = 11.34 ppm), and the pyrrole-βH (δ = 9.59 ppm) of the porphyrin subunit-**1-Zn** in capsule **2•1-Zn•2** were shifted downfield by 0.12, 0.01, and 0.19 ppm, respectively, relative to those of the subunit-**1** in **2•1•2**.

It is known that the one-point hydrogen bond between phenol and pyridine is very weak,[8] compared with the coordination bond between Zn-tetraphenylporphyrin and pyridine.[9,10] However, this is not the case for the association between **1-Zn** and **2**. Thus, cooperative and double quadruple ArOH···Npy hydrogen bonds

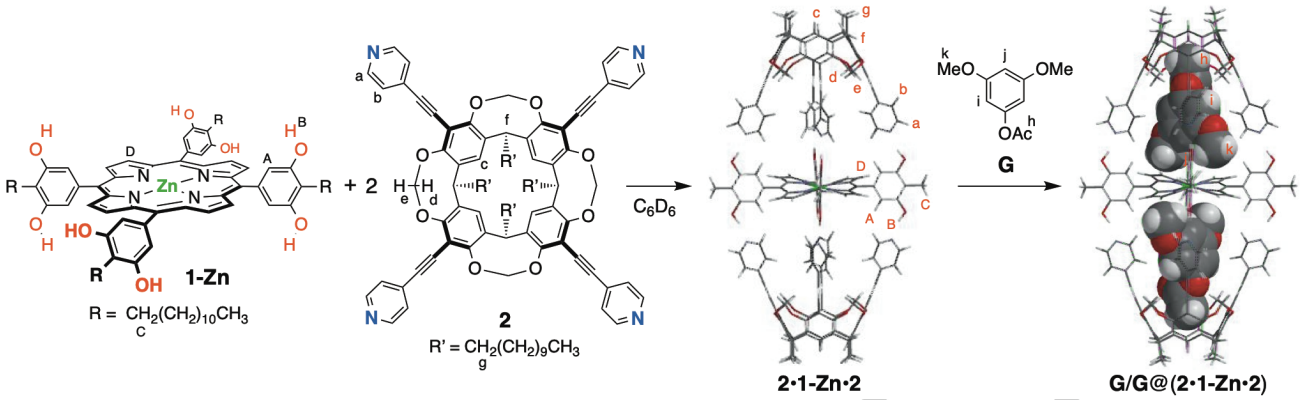

Scheme 2. Self-assembly of a 1:2 mixture of **1-Zn** and **2** into **2•1-Zn•2** and its guest encapsulation to form **G**/**G**@(**2•1-Zn•2**). Molecular models are calculated at the PM3 level, wherein the dodecyl side chains of the subunit-**1-Zn** and the undecyl side chains of the subunit-**2** are replaced by methyl groups.

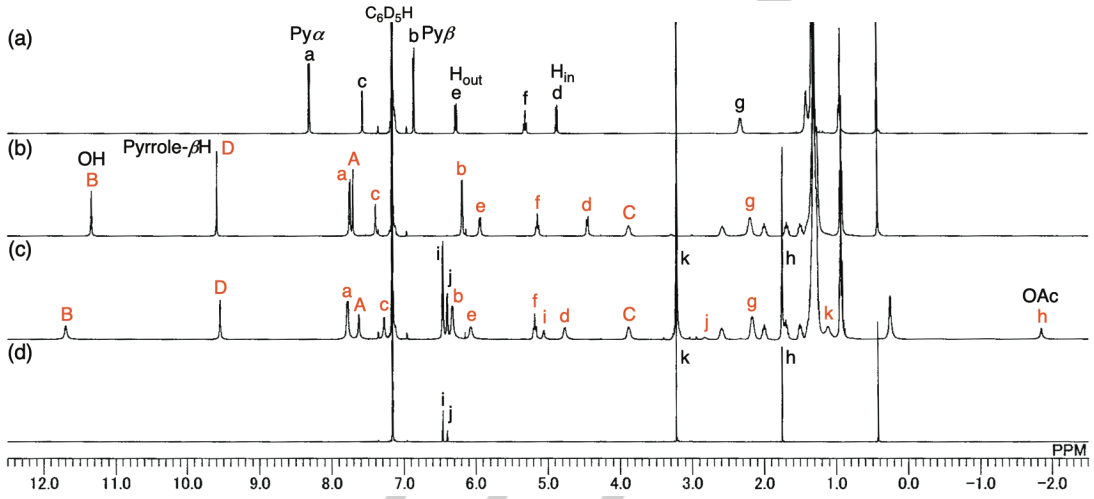

Figure 2. ^{1}H NMR spectra (400 MHz, C_6D_6, 298 K) of (a) **2** alone, (b) **2•1-Zn•2** (after heating [**1-Zn**] = 2 mM if soluble and [**2**] = 4 mM at 70 °C for 12 h), (c) **G**/**G**@(**2•1-Zn•2**) and free **G** ([**2•1-Zn•2**] = 2 mM and [**G**] = 17 mM), and (d) **G** alone. The signals marked 'A-D' and 'a-k' are assigned in Figure 1 and Scheme 2. The signals of free species and complexes are shown in black and red, respectively.

between **1-Zn** and two molecules of **2** are much more favorable than the Zn–Npy coordination bond between **1-Zn** and **2**, and play an important role in the formation of the thermodynamically stable hydrogen-bonded **2•1-Zn•2**.[6b,11]

Guest Encapsulation of Capsule 2•1-Zn•2

Previously, we reported the encapsulation of two molecules of 1-acetoxy-3,5-dimethoxybenzene (**G**) as a guest in capsule **2•1•2** to form **G**/**G**@(**2•1•2**) in C_6D_6, with accommodation of one **G** in each cavity.[6a] When 1 equiv. of **G** was added to **2•1•2** in C_6D_6, capsule **G**@(**2•1•2**) with one molecule encapsulation of **G** was detected concomitantly with **G**/**G**@(**2•1•2**) and free **2•1•2**, in which the ^{1}H NMR NH and OH signals of these three species were observed independently (Figure S3 in the Supporting Information).[6a] In a manner similar to **2•1•2**, capsule **2•1-Zn•2** also encapsulated two molecules of **G**, wherein the ^{1}H NMR signals of **G**/**G**@(**2•1-Zn•2**) and free **G** were independently observed because of the slow exchange of **G** in and out of **2•1-Zn•2** on the NMR time scale (Figure 2c vs. 2d, Figure S4, and Scheme 2). The ^{1}H NMR chemical shift changes of the signals of the encapsulated **G** relative to those of free **G** ($\Delta\delta = \delta_{\text{encapsulated-guest}} - \delta_{\text{free-guest}}$) were –1.41, –3.57, –2.10, and –3.60 ppm for ArH_{ortho}, ArH_{para}, OMe, and OAc protons of the encapsulated **G**, respectively, due to the shielding effects of **2•1-Zn•2** (Table S2). The OAc signal of the encapsulated **G** appeared at $\delta = -1.85$ ppm. These $\Delta\delta$ values and a molecular model of **G**/**G**@(**2•1-Zn•2**) show that the methyl groups of the OMe groups at the *meta*-positions of the encapsulated **G** are oriented to the porphyrin ring of the subunit-**1-Zn** and the methyl group of the OAc group of the encapsulated **G** is oriented to the bowl-shaped aromatic cavity of the subunit-**2**, via guest–host CH–π (van der Waals) interactions (Scheme 2).

In the ^{1}H NMR spectra, guest-encapsulation behaviors of **2•1-Zn•2** are somewhat different from those of **2•1•2** as follows. (1) For the chemical shift values of the encapsulated **G**, the signals of OAc and ArH_{ortho} protons in **G**/**G**@(**2•1-Zn•2**) were slightly shifted upfield by 0.02 and 0.04 ppm, respectively, relative to those of **G**/**G**@(**2•1•2**), whereas the signals of OMe and ArH_{para} protons in **G**/**G**@(**2•1-Zn•2**) were shifted downfield by 0.19 and 0.05 ppm, respectively, relative to those of **G**/**G**@(**2•1•2**) (Table S2). (2) In contrast to **2•1•2**,[6a] one molecular **G**-encapsulated capsule **G**@(**2•1-Zn•2**) was not observed, and only **G**/**G**@(**2•1-Zn•2**) and free **2•1-Zn•2** were observed upon addition of 1–3

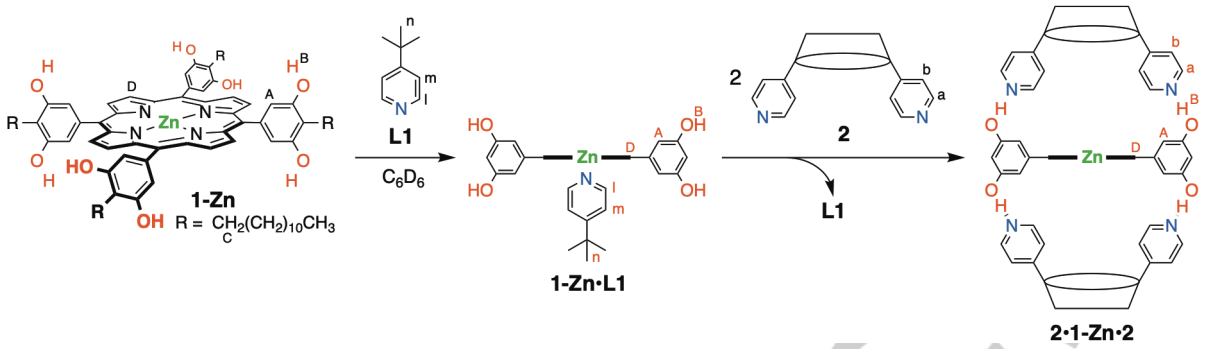

Scheme 3. Formation of **1-Zn•L1** from a 1:1 mixture of **1-Zn** and **L1**, and formation of **2•1-Zn•2** concomitantly with release of **L1** upon addition of 2 equiv. of **2** to **1-Zn•L1**.

equiv. of **G** (Figure S5), wherein the ^{1}H NMR OH signals of only the two species were observed. (3) When assuming that a mixture of **2•1•2** and **G** does not contain **G**@(**2•1•2**), the apparent association constant (K_{app}) of **2•1•2** with **G** to form **G**/**G**@(**2•1•2**) was $K_{app} \geq 1.0 \times 10^7$ M^{-2} in C_6D_6 at 298 K,[6a] whereas the association constant (K_a) of **2•1-Zn•2** with **G** to form **G**/**G**@(**2•1-Zn•2**) was estimated to be 3.2×10^5 M^{-2} in C_6D_6 at 298 K based on the signal integrations between free **2•1-Zn•2** and **G**/**G**@(**2•1-Zn•2**) as a function of the concentration of **G** (Figure S5).

Behavior of Capsule 2•1-Zn•2 when It Associates with Pyridyl Ligands

It is known that Zn-*meso*-tetraarylporphyrin can bind a pyridyl compound as an axial ligand through a Zn–Npy coordination bond.[9,10] We chose 4-*tert*-butylpyridine (**L1**) and 4-(4-methylphenyl)pyridine (**L2**) (Figure 1). The molecular length of **L2** is similar to the cavity length of **2•1-Zn•2**, but the molecular length of **L1** is shorter than that of **2•1-Zn•2**.

The behavior of **L1** when it associates with **1-Zn** or **2•1-Zn•2** was monitored by ^{1}H NMR and is shown in Figure S6. Zn-porphyrin **1-Zn** alone is not soluble in C_6D_6. However, a 1:1 mixture of **1-Zn** and **L1** becomes soluble in C_6D_6 after heating the mixture at 70 °C for 12 h. In this mixture, the ^{1}H NMR OH signal of **1-Zn** appeared at 4.37 ppm, and the signals of the Pyβ-proton and the *t*-butyl group of **L1** were shifted upfield by 1.23 and 0.73 ppm, respectively, relative to those of free **L1** (Figure S6b vs. S6a), owing to the ring-current effect of **1-Zn**, although the signal of the Pyα-proton was not observed. This result indicates that **1-Zn** binds **L1** to form **1-Zn•L1** through Zn–Npy coordination bond, but not ArOH···Npy hydrogen bond. Upon addition of 2 equiv. of **2** to this mixture, the signals of capsule **2•1-Zn•2** and free-like **L1** were observed (Figure S6c vs. S6b, S6a, and S6f). This result suggests the release of **L1** from **1-Zn•L1** upon formation of **2•1-Zn•2** (Scheme 3), probably because C_6D_6-encapsulating **2•1-Zn•2** is thermodynamically more stable than **L1**-encapsulating **2•1-Zn•2**. Upon addition of 8.5 equiv. of **G** to this mixture, the signals of **G**/**G**@(**2•1-Zn•2**), free **L1**, and excess free **G** were observed (Figure S6d vs. S6c, S6a, and S6e). Thus, **G**/**G**@(**2•1-Zn•2**) is thermodynamically most stable among them.

The behavior of **L2** when it associates with **1-Zn** or **2•1-Zn•2** was monitored by ^{1}H NMR and is shown in Figure 3. A 1:1 mixture of **1-Zn** and **L2** becomes soluble in C_6D_6 after heating the mixture at 70 °C for 12 h. In this mixture, the ^{1}H NMR OH signal of **1-Zn** appeared at 4.45 ppm, and the signal of the methyl group of **L2** was shifted upfield by 0.12 ppm relative to that of free **L2** (Figure 3b vs. 3a), although the signals of the Pyα- and Pyβ-protons were not observed, probably due to highly broadened signals. This result suggests that **1-Zn** binds **L2** to form **1-Zn•L2** through Zn–Npy coordination bond, but not ArOH···Npy hydrogen bond (Scheme 4A). Upon addition of 2 equiv. of **2** to this mixture, the signal of the methyl group of **L2** was broadened and shifted highly upfield by 3.68 ppm (δ = –1.57 ppm) relative to that of free **L2**, and the broadened OH signals of subunit-**1-Zn** appeared at 11.35 and 10.63 ppm in a 2.6:1 integration ratio, and shifted highly downfield by 6.90 and 6.18 ppm, respectively, relative to that of **1-Zn•L2** (Figure 3c vs. 3b). These results strongly suggest the formation of capsule **2•1-Zn•2** and the encapsulation of **L2** in **2•1-Zn•2** in a mole ratio of **2•1-Zn•2**:**L2**@(**2•1-Zn•2**) = (2.6 – 1)/2:1 = 0.8:1 (Scheme 4A). The highly upfield-shifted signal of the methyl group of **L2** arises from the shielding effect of the aromatic cavity end of the bowl-shaped subunit-**2**, wherein the molecular size of **L2** fits the cavity size of **2•1-Zn•2** to interact with each other by CH–π interaction. In **L2**@(**2•1-Zn•2**), two OH signals were observed because of structural desymmetrization by the encapsulation of **L2**, in which the OH signal of the **L2**@(**2•1-Zn**) moiety (δ = 10.63 ppm) would be shifted more upfield, due to the shielding effect of **L2**, than that of the **1-Zn•2** moiety (δ = 11.35 ppm). The OH signal of **2•1-Zn•2** appears at 11.34 ppm, as mentioned above (Figures 2b and 3f). Thus, the OH signal at δ = 11.35 ppm would be an overlap of the OH signal of **2•1-Zn•2** and that of the **1-Zn•2** moiety in **L2**@(**2•1-Zn•2**).

Simultaneous Encapsulation of Guest and Pyridyl Ligand in Capsule 2•1-Zn•2

We found preferential simultaneous encapsulation of **G** and **L2** in **2•1-Zn•2** to form **G**/**L2**@(**2•1-Zn•2**), as shown in Schemes 1A and 4B. Figure 3d shows the ^{1}H NMR spectrum of the mixture at 298 K after heating a 1:1:8.5 mixture of capsule **2•1-Zn•2** (2 mM), **L2**, and **G** in C_6D_6 at 70 °C for 12 h. Figure S7 shows the 2D NOESY spectrum under the same conditions of Figure 3d. The signal of the OAc group of the encapsulated **G** appeared at –1.84 ppm ($\Delta\delta$ = –3.59 ppm), and the signal of the methyl group of the encapsulated **L2** sharpened, as compared with **L2** in **L2**@(**2•1-Zn•2**), and appeared at –1.57 ppm ($\Delta\delta$ = –3.68 ppm) (Figure 3d vs. 3c). The OH signals of subunit-**1-Zn** also sharpened, as compared with **L2**@(**2•1-Zn•2**), and appeared at 11.66, 11.62, and 10.65 ppm. The OH signal of subunit-**1-Zn** and the signal of the OAc group of the encapsulated **G** in **G**/**G**@(**2•1-Zn•2**) appear at 11.69 and –1.85 ppm ($\Delta\delta$ = –3.60 ppm), as mentioned above (Figures 2c and 3e). Thus, the OH signal of subunit-**1-Zn** at 11.66

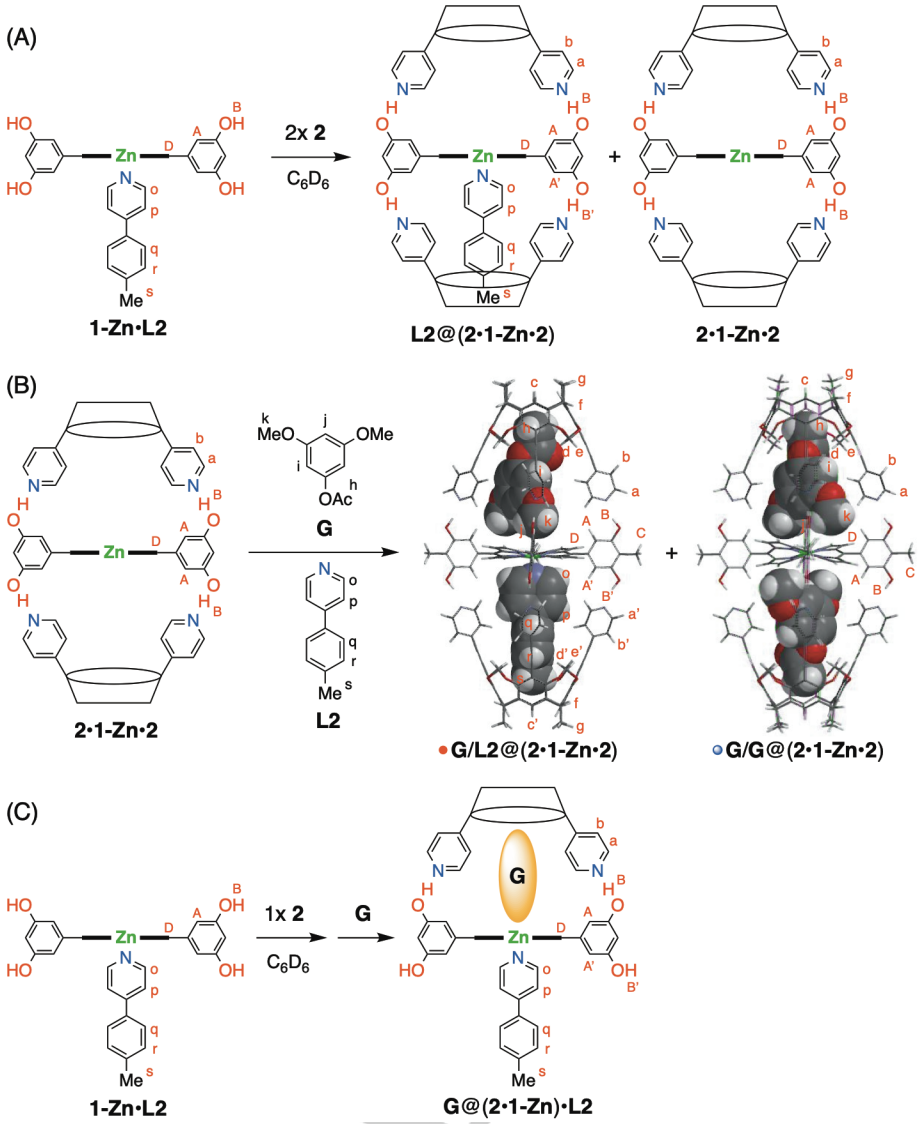

Scheme 4. (A) Formation of **1-Zn•L2** from a 1:1 mixture of **1-Zn** (2 mM) and **L2**, and formation of a mixture of **L2@(2•1-Zn•2)** and **2•1-Zn•2** in a 1:0.8 mole ratio upon addition of 2 equiv. of **2** to **1-Zn•L2**. (B) Formation of a mixture of **G/L2@(2•1-Zn•2)** and **G/G@(2•1-Zn•2)** in a 52:48 or 91:9 mole ratio from a 1:1:8.5 or 1:8.5:8.5 mixture of **2•1-Zn•2** (2 mM), **L2**, and **G**, respectively. (C) Formation of **G@(2•1-Zn)•L2** as a major assembly from a 1:1:1:8.5 mixture of **1-Zn** (2 mM), **L2**, **2**, and **G**. Molecular models in Scheme 4B are calculated at the PM3 level, wherein the dodecyl side chains of the subunit-**1-Zn** and the undecyl side chains of the subunit-**2** are replaced by methyl groups.

ppm and the signal of the OAc group of the encapsulated **G** at –1.84 ppm in Figure 3d correspond to **G/G@(2•1-Zn•2)**. However, the integration value of the signal of the OAc group of the encapsulated **G** at –1.84 ppm was larger than that of the encapsulated **G** in **G/G@(2•1-Zn•2)**. This result suggests that the signal of the OAc group of the encapsulated **G** at –1.84 ppm in **G/G@(2•1-Zn•2)** overlaps with that of the encapsulated **G** in another new species. Based on the **L2** encapsulation and the 1:1 integration ratio of the OH signals of subunit-**1-Zn** at 11.62 and 10.65 ppm, another new species in Figure 3d was found to be **G/L2@(2•1-Zn•2)** with simultaneous encapsulation of **G** and **L2** (Scheme 4B). In **G/L2@(2•1-Zn•2)**, the capsule structure is desymmetrized by the simultaneous encapsulation of **G** and **L2**, in which the OH signal of the **L2@(2•1-Zn)** moiety (δ = 10.65 ppm) would be shifted more upfield, due to the shielding effect of **L2**, than that of the **G@(2•1-Zn)** moiety (δ = 11.62 ppm). Based on the comparison of the integration values of the OH signals of **G/L2@(2•1-Zn•2)** with that of **G/G@(2•1-Zn•2)**, and comparison of the integration value of the signal of the methyl group of the encapsulated **L2** in **G/L2@(2•1-Zn•2)** with that of the overlapped signals of the OAc groups of the encapsulated **G** in **G/L2@(2•1-Zn•2)** and **G/G@(2•1-Zn•2)**, the formation ratio of **G/L2@(2•1-Zn•2)** and **G/G@(2•1-Zn•2)** was estimated to be 52:48 under the conditions of a 1:1:8.5 mixture of capsule **2•1-Zn•2** (2 mM), **L2**, and **G** in C_6D_6 at 298 K. The signal of the pyrrole-βH (δ = 9.54 ppm) of the subunit-**1-Zn** in **G/L2@(2•1-Zn•2)** overlapped with that (δ = 9.54 ppm) in **G/G@(2•1-Zn•2)**.

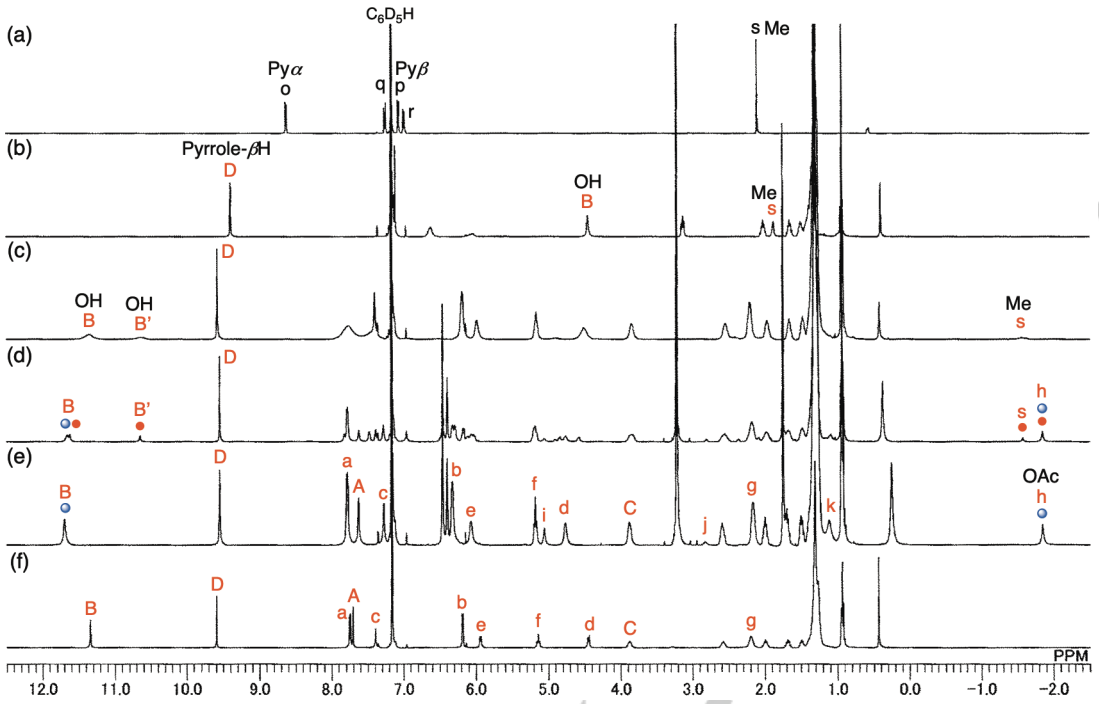

Figure 3. Association behavior of **2•1-Zn•2** and **L2** in the absence or presence of **G**, monitored by ^{1}H NMR (400 MHz, C_6D_6, 298 K): (a) **L2** alone, (b) [**1-Zn**] = [**L2**] = 2 mM after heating at 70 °C for 12 h, (c) [**2•1-Zn•2**] = [**L2**] = 2 mM after heating at 70 °C for 12 h, (d) [**2•1-Zn•2**] = [**L2**] = 2 mM and [**G**] = 17 mM after heating at 70 °C for 12 h, (e) [**2•1-Zn•2**] = 2 mM and [**G**] = 17 mM, and (f) [**2•1-Zn•2**] = 2 mM. The signals marked 'A-D' and 'a-k and o-s' are assigned in Figure 1 and Scheme 4. The representative signals of **G**/**G**@(**2•1-Zn•2**) and **G**/**L2**@(**2•1-Zn•2**) are shown in blue and red circles, respectively.

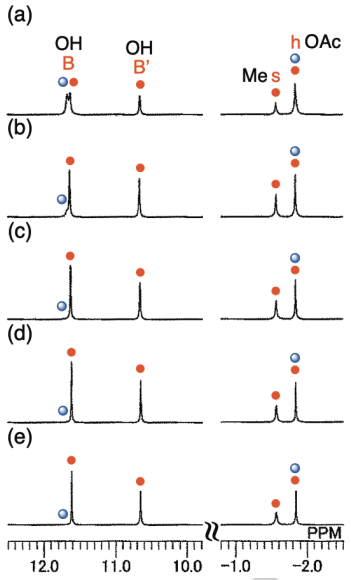

Figure 4. ^{1}H NMR spectral changes (400 MHz, C_6D_6, 298 K) of a 1:8.5 mixture of capsule **2•1-Zn•2** (2 mM) and **G** (17 mM) (constant) upon addition of **L2** (1–25.5 equiv.) in the region of the OH signals of subunits-**1-Zn** and in the region of the signals of the OAc groups of **G** and the methyl group of **L2** encapsulated in **G**/**G**@(**2•1-Zn•2**) and **G**/**L2**@(**2•1-Zn•2**): (a) [**L2**] = 2 mM, (b) [**L2**] = 6 mM, (c) [**L2**] = 17 mM, (d) [**L2**] = 34 mM, and (e) [**L2**] = 51 mM. The representative signals of **G**/**G**@(**2•1-Zn•2**) and **G**/**L2**@(**2•1-Zn•2**) are shown in blue and red circles, respectively.

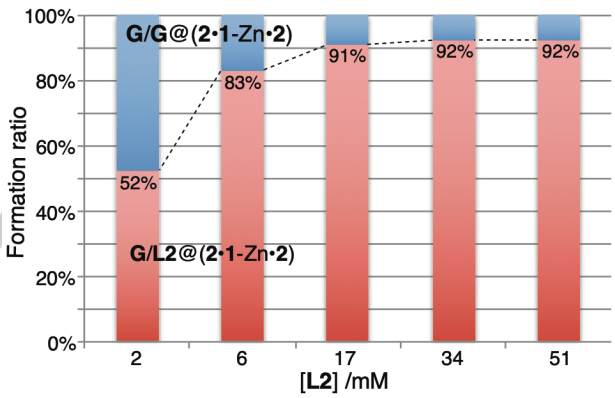

Figure 5. Plots of the formation ratio of **G**/**L2**@(**2•1-Zn•2**) and **G**/**G**@(**2•1-Zn•2**) as a function of the concentration of **L2** in C_6D_6 at 298 K under the condition of [**2•1-Zn•2**] = 2 mM and [**G**] = 17 mM (constant), based on the ^{1}H NMR data of Figure 4.

Figure 4 shows the ^{1}H NMR spectral changes of a 1:8.5 mixture of capsule **2•1-Zn•2** (2 mM, constant) and **G** (17 mM, constant) upon addition of 1–25.5 equiv. of **L2** (2–51 mM) in C_6D_6 at 298 K in the region of the OH signals of subunit-**1-Zn** and in the region of the signals of the OAc groups of **G** and the methyl group of **L2** encapsulated in **G**/**G**@(**2•1-Zn•2**) and **G**/**L2**@(**2•1-Zn•2**) (Scheme 4B). The full spectra of Figure 4 are shown in Figure S8. Figure 5 shows the plots of the formation ratio of **G**/**L2**@(**2•1-Zn•2**) to **G**/**G**@(**2•1-Zn•2**) as a function of the concentration of **L2** in C_6D_6 at 298 K, based on the ^{1}H NMR data presented in Figure 4. The formation ratio of **G**/**L2**@(**2•1-Zn•2**) to **G**/**G**@(**2•1-Zn•2**) increased with increasing the concentration of **L2** and reached

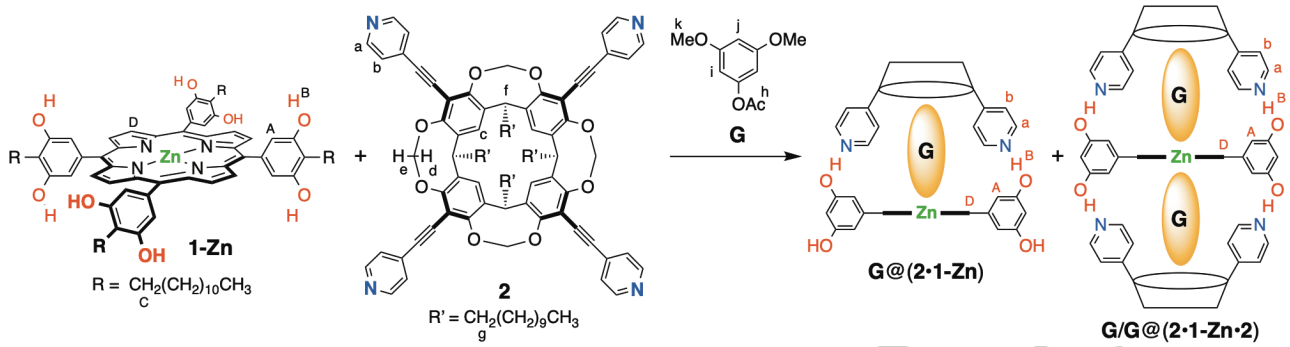

Scheme 5. Formation of **G**@(**2•1-Zn**) as a major assembly and **G**/**G**@(**2•1-Zn•2**) as a minor assembly from a 1:1:8.5 mixture of **1-Zn** (2 mM), **2**, and **G**.

91:9 and steady state of 92:8 upon addition of 17 and 34 mM, respectively, of **L2**. Thus, the preferential simultaneous encapsulation of **G** and **L2** in **2•1-Zn•2** to form **G**/**L2**@(**2•1-Zn•2**) was achieved. Figure S9 shows the 2D NOESY spectrum under the same conditions of a 1:17:8.5 mixture of capsule **2•1-Zn•2** (2 mM), **L2**, and **G** (Figure 4d and Figure S8d), in which the ^{1}H NMR signals of **G**/**L2**@(**2•1-Zn•2**) were assigned. The exchange cross-peaks between the signals of the two OH groups of the subunit-**1-Zn** and H_2O, between the signals of the encapsulated and free **L2**, and between the signals of the encapsulated and free **G** are observed in Figure S9. Even upon addition of an excess amount of **L2**, (1) the chemical shift values of the signals of the two OH groups of the subunit-**1-Zn** in **G**/**L2**@(**2•1-Zn•2**) remained unchanged, and (2) the signals of the encapsulated and free **L2** and **G** were observed independently (not averaged; Figure 4 and Figure S8). These results indicate that **G**/**L2**@(**2•1-Zn•2**) is thermodynamically stable even in the presence of the excess amount of **L2**. As indicated above, cooperative and double quadruple ArOH···Npy hydrogen bonds between **1-Zn** and two molecules of **2** are much more favorable than one-point ArOH···Npy hydrogen bond between **1-Zn** and **L2**, and play an important role in the formation of the thermodynamically stable hydrogen-bonded **2•1-Zn•2**.[6b,8,11]

Half-Capsule 2•1-Zn

As mentioned above, a 1:1:2 mixture of **1-Zn**, **L2**, and **2** in the absence or presence of **G** self-assembles into a mixture of **L2**@(**2•1-Zn•2**) and **2•1-Zn•2** (Figure 3c) or a mixture of **G**/**L2**@(**2•1-Zn•2**) and **G**/**G**@(**2•1-Zn•2**) (Figure 3d), respectively. Figure S10 shows the ^{1}H NMR spectra of a 1:1:1 mixture of **1-Zn**, **L2**, and **2** (2 mM each) in the absence or presence of **G** to form a half-capsule (**2•1-Zn**)•**L2** or **G**@(**2•1-Zn**)•**L2**, respectively, as shown in Scheme 4C. A 1:1 mixture of **1-Zn** and **L2** self-assembles into **1-Zn•L2** through Zn–Npy coordination bond (Figure S10b and Figure 3b), in which the signals of the pyrrole-βH and the OH group of the subunit-**1-Zn** appeared at 9.39 and 4.45 ppm, respectively. Upon addition of 1 equiv. of **2** to this mixture, the signals of the pyrrole-βH of the subunit-**1-Zn** shifted at 9.42 ppm with a shoulder peak at ca. 9.48 ppm, and the OH signals appeared at 11.39 ppm and at ca. 4.45 ppm, but the signal of the methyl group of the encapsulated **L2** was not observed at around –1.57 ppm (Figure S10c vs. Figure 3c). These results may suggest that a 1:1:1 mixture of **1-Zn**, **L2**, and **2** self-assembles preferentially into a half-capsule (**2•1-Zn**)•**L2** with coordination of **L2** at the outer side of **2•1-Zn**.[6b] In a 1:1:1:8.5 mixture of **1-Zn**, **L2**, **2**, and **G**, the signals of the pyrrole-βH of the subunit-**1-Zn** appeared at 9.44 ppm as a major component and at 9.52 ppm as a minor component, the OH signals appeared at 11.68 ppm as a major component and at 10.68 ppm as a minor component, and the signals of the OAc group of the encapsulated **G** appeared at –1.89 ppm with a shoulder peak at ca. –1.86 ppm and the signal of the methyl group of the encapsulated **L2** appeared at –1.58 ppm as a minor component (Figure S10d vs. Figure 3d). These results suggest the formation of the **G**-encapsulating half-capsule **G**@(**2•1-Zn**)•**L2** as a major assembly (Scheme 4C),[6b] together with **G**/**L2**@(**2•1-Zn•2**) and **G**/**G**@(**2•1-Zn•2**) as minor assemblies.

Figure S11 shows the ^{1}H NMR spectra of a 1:1 mixture of **1-Zn** and **2** (2 mM each) in the absence or presence of **G** without **L2**. In a 1:1: mixture of **1-Zn** and **2** (Figure S11b), the signal of the pyrrole-βH of the subunit-**1-Zn** appeared at 9.44 ppm, which was between the values of half-capsule **2•3-Zn** (δ = 9.36 ppm)[6b] and capsule **2•1-Zn•2** (δ = 9.59 ppm). These results suggest that the signal of the pyrrole-βH of the subunit-**1-Zn** was observed as an averaged form of an equilibrium mixture of **1-Zn•2** and **2•1-Zn•2**. In a 1:1:8.5 mixture of **1-Zn**, **2**, and **G**, the signals of the pyrrole-βH of the subunit-**1-Zn** appeared at 9.37 ppm with a shoulder peak at ca. 9.48 ppm, the OH signal appeared at 11.68 ppm, and the signal of the OAc group of the encapsulated **G** appeared at –1.89 ppm (Figures S11c and S10e). It is known that the signal of the pyrrole-βH of **G**@(**2•3-Zn**)[6b] or **G**/**G**@(**2•1-Zn•2**) appears at 9.34 or 9.54 ppm, respectively. These results suggest the formation of **G**@(**2•1-Zn**) as a major assembly, together with **G**/**G**@(**2•1-Zn•2**) as a minor assembly (Scheme 5).

Doubly Cavitand-Capped Double-Decker Zn-Porphyrin Capsule 2•1-Zn•L3•1-Zn•2

As mentioned above, a 1:1:1 mixture of **1-Zn**, **L2**, and **2** (2 mM each) in the absence or presence of **G** self-assembles into a half-capsule (**2•1-Zn**)•**L2** or **G**@(**2•1-Zn**)•**L2**, respectively, in which **L2** coordinates to half-capsule **2•1-Zn** at the outer side of **2•1-Zn**, as shown in Scheme 4C. It is known that **L3** (DABCO) serves as a ditopic ligand to connect two Zn-porphyrins.[12,13] Thus, when **L3** is used in place of **L2**, it is expected to form doubly cavitand-capped double-decker Zn-porphyrin capsule **2•1-Zn•L3•1-Zn•2**, in which two half-capsules **2•1-Zn** are connected by **L3** through **1-Zn•L3•1-Zn** coordination bonds and by the assistance of ArOH···OH(Ar) hydrogen bonds between two **1-Zn** subunits (Scheme 1B).[13,14]

Figure 6b and 6c show the ^{1}H NMR spectra of a 2:1:2 mixture of **1-Zn** (2 mM if soluble), **L3**, and **2** in C_6D_6 at 298 K in the absence and presence of **G**, respectively. A 2:1 mixture of **1-Zn** and **L3** (1 mM) was almost insoluble in C_6D_6 even after heating

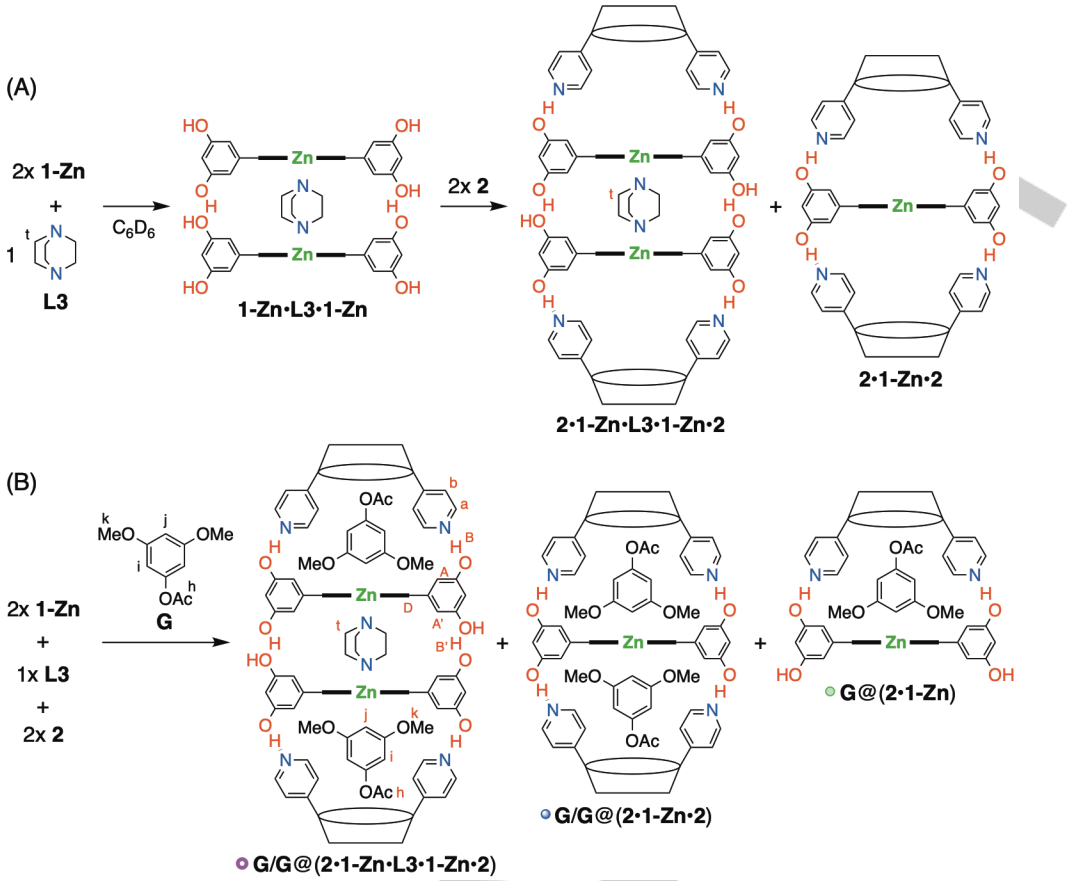

Scheme 6. (A) Formation of a mixture of **2•1-Zn•L3•1-Zn•2** and **2•1-Zn•2** from a 2:1:2 mixture of **1-Zn**, **L3**, and **2**. (B) Formation of a mixture of **G**/**G**@(**2•1-Zn•L3•1-Zn•2**), **G**@(**2•1-Zn**), and **G**/**G**@(**2•1-Zn•2**) in a 1.00:0.61:0.18 mole ratio from a 2:1:2:17 mixture of **1-Zn** (2 mM), **L3**, **2**, and **G**.

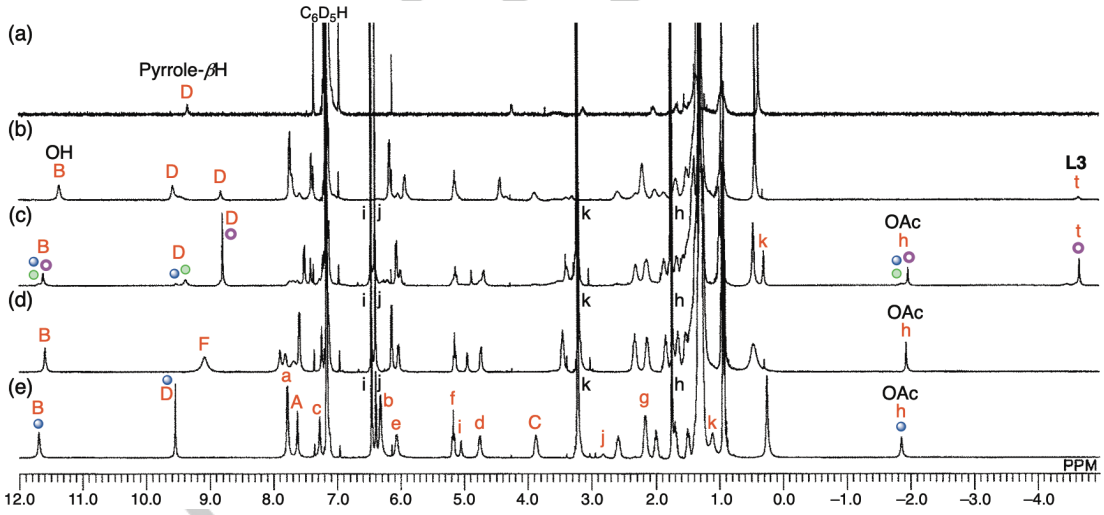

Figure 6. ^{1}H NMR spectra (400 MHz, C_6D_6, 298 K) of (a) [**1-Zn**] = 2 mM and [**L3**] = 1 mM after heating at 70 °C for 12 h, (b) [**1-Zn**] = [**2**] = 2 mM and [**L3**] = 1 mM after heating at 70 °C for 12 h, (c) [**1-Zn**] = [**2**] = 2 mM, [**L3**] = 1 mM, and [**G**] = 17 mM after heating at 70 °C for 12 h, (d) [**2**] = [**3-Zn**] = 2 mM, [**L3**] = 1 mM, and [**G**] = 17 mM, and (e) **G**/**G**@(**2•1**-Zn•**2**) and free **G**. The signals marked 'A-F' and 'a-k and t' are assigned in Figure 1 and Schemes 1B and 6 or Scheme 7. The signals of free **G** and complexes are shown in black and red, respectively. The representative signals of **G**/**G**@(**2•1-Zn•L3•1-Zn•2**), **G**@(**2•1-Zn**), and **G**/**G**@(**2•1-Zn•2**) are shown in purple open circle, light green circle, blue circle, respectively.

this mixture at 70 °C for 12 h (Figure 6a). However, a 2:1:2 mixture of **1-Zn**, **L3**, and **2** became soluble in C_6D_6 after heating the mixture at 70 °C for 12 h (Figure 6b; addition of **2** to a 2:1 mixture of **1-Zn** and **L3**). The two broadening signals of the pyrrole-βH of the subunit-**1-Zn** appeared at 9.57 and 8.81 ppm, the OH signal appeared at 11.36 ppm, and the broadening signal

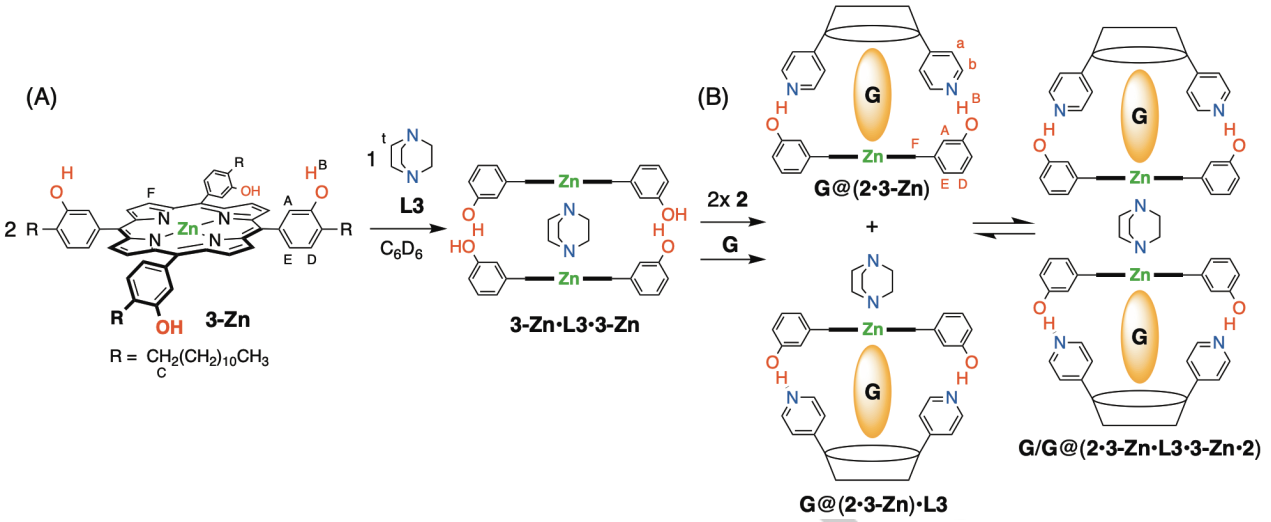

Scheme 7. (A) Formation of an equilibrium mixture of **3-Zn•L3•3-Zn**, **3-Zn•L3**, **3-Zn**, and **L3** from a 2:1 mixture of **3-Zn** and **L3**. (B) Formation of an equilibrium mixture of **G**/**G@(2•3-Zn•L3•3-Zn•2)**, **G@(2•3-Zn)•L3**, **G@(2•3-Zn)**, and **L3** from a 2:1:2:17 mixture of **3-Zn**, **L3**, **2**, and **G**.

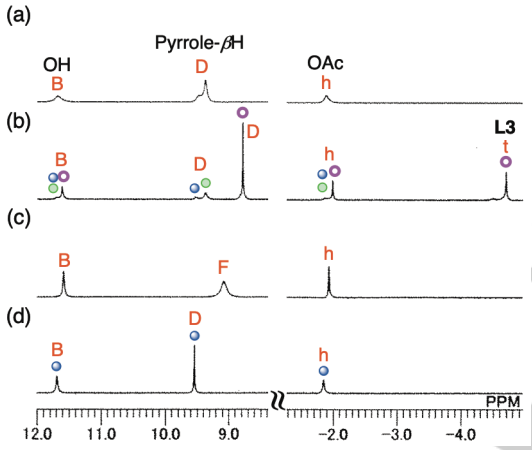

Figure 7. ^{1}H NMR spectra (400 MHz, C_6D_6, 298 K) in the region of the OH and the pyrrole-βH signals of subunits-**1-Zn** and in the region of the signals of the OAc groups of the encapsulated **G** and the methylene group of the encapsulated **L3**: (a) [**1-Zn**] = [**2**] = 2 mM and [**G**] = 17 mM, (b) [**1-Zn**] = [**2**] = 2 mM, [**L3**] = 1 mM, and [**G**] = 17 mM, (c) [**2**] = [**3-Zn**] = 2 mM, [**L3**] = 1 mM, and [**G**] = 17 mM, and (d) **G**/**G@(2•1-Zn•2)** and free **G**. The signals marked 'B and D or F' and 'h and t' are assigned in Figure 1 and Schemes 1B and 6 or Scheme 7, respectively. The representative signals of **G/G@(2•1-Zn•L3•1-Zn•2)**, **G@(2•1-Zn)**, and **G/G@(2•1-Zn•2)** are shown in purple open circle, light green circle, blue circle, respectively.

of **L3** appeared at –4.68 ppm ($\Delta\delta$ = –7.12 ppm) (Figure 6b). As mentioned above, the signal of the pyrrole-βH in **2•1-Zn•2** appears at 9.59 ppm. The signal of the pyrrole-βH at 9.57 ppm indicates the formation of **2•1-Zn•2**. The signal of the pyrrole-βH at 8.81 ppm was shifted upfield by 0.78 and 0.55 ppm relative to those of capsule **2•1-Zn•2** (δ = 9.59 ppm) and a half-capsule **2•3-Zn** (δ = 9.36 ppm),[6b] respectively, due to the mutual shielding effect of two proximal **1-Zn** subunits.[12b,13] Moreover, the signal of **L3** was largely shifted upfield by 7.12 ppm relative to free **L3**, due to the strong shielding effect (ring-current effect) based on the encapsulation of **L3** between two proximal **1-Zn** subunits.[12,13] These results strongly indicate the formation of capsule **2•1-Zn•L3•1-Zn•2**. Thus, a 2:1:2 mixture of **1-Zn**, **L3**, and **2** self-assembles into a mixture of **2•1-Zn•L3•1-Zn•2** and **2•1-Zn•2** (Scheme 6A). Figure 6c shows a 2:1:2:17 mixture of **1-Zn**, **L3**, **2**, and **G** after heating the mixture at 70 °C for 12 h (addition of **G** to a 2:1:2 mixture of **1-Zn**, **L3**, and **2**). Upon addition of **G**, the signals derived from **2•1-Zn•L3•1-Zn•2** sharpened (Figure 6c vs. 6b). The signals of the pyrrole-βH and the OH group of the subunit-**1-Zn** appeared at 8.79 and 11.62 ppm, respectively. The signal of the OAc group of the encapsulated **G** and the signal of the encapsulated **L3** appeared at –1.99 and –4.69 ppm, respectively. The mole ratio of the encapsulated **G** and **L3** was found to be 2:1 based on the comparison between their signal integrations. Thus, a 2:1:2:17 mixture of **1-Zn**, **L3**, **2**, and **G** self-assembles into **G/G@(2•1-Zn•L3•1-Zn•2)** as a major assembly (Schemes 1B and 6B). In the 2D NOESY spectrum under the same conditions of Figure 6c, exchange cross-peaks were observed between the H_2O signal and the signals at 11.62 and ca. 6.39 ppm (Figure S12). The OH group at 11.62 ppm indicates the ArOH···Npy hydrogen bonds between the subunit-**1-Zn** and the subunit-**2**. The OH group at ca. 6.39 ppm suggests ArOH···OH(Ar) hydrogen bonds between two **1-Zn** subunits (Scheme 6B).[13,14] As minor assemblies, the signals of the pyrrole-βH of the subunit-**1-Zn** also appeared at 9.52 and 9.37 ppm, which correspond to **G/G@(2•1-Zn•2)** (Figures 2c and 6e) and **G@(2•1-Zn)** (Figures S11c and S10e), respectively, as mentioned above. Based on the integration ratio of the signals of the pyrrole-βH of the subunit-**1-Zn** at 8.79, 9.37, and 9.52 ppm, the formation ratio of **G/G@(2•1-Zn•L3•1-Zn•2)**, **G@(2•1-Zn)**, and **G/G@(2•1-Zn•2)** was found to be 1.00:0.61:0.18 (Scheme 6B).

To evaluate the importance of ArOH···OH(Ar) hydrogen bonds between two **1-Zn** subunits in the self-assembly of **G/G@(2•1-Zn•L3•1-Zn•2)**, the ^{1}H NMR study using soluble **3-Zn**[6b] in C_6D_6 in place of **1-Zn** was conducted (Figure S13 and Figure 6d).

A 2:1 mixture of **3-Zn** and **L3** was soluble in C_6D_6, and the signal of the pyrrole-βH of the subunit-**3-Zn** appeared at 8.96 ppm. This value was shifted upfield by 0.33 ppm relative to that of **3-Zn** alone (Figure S13b vs. S13a). This result suggests the formation of double-decker Zn-porphyrin **3-Zn•L3•3-Zn**, in which two **3-Zn** subunits are connected by **L3** coordination bonds and the

assistance of ArOH···OH(Ar) hydrogen bonds between two **3-Zn** subunits (Scheme 7A). The signals of **L3** and the OH group of the subunit-**3-Zn** were not observed (Figure S13b), probably due to fast exchanges on the NMR time scale between **3-Zn•L3•3-Zn** and **3-Zn•L3** + **3-Zn** or between **3-Zn•L3** and **3-Zn** + **L3**. In a 2:1:2 mixture of **3-Zn**, **L3**, and **2**, the signals of the pyrrole-βH and the OH group of the subunit-**3-Zn** appeared at 9.18 and 11.36 ppm, respectively, but the signal of **L3** was not observed (Figure S13c).

In a 2:1:2:17 mixture of **3-Zn**, **L3**, **2**, and **G**, the signals of the pyrrole-βH and the OH group of the subunit-**3-Zn** appeared at 9.09 and 11.59 ppm, respectively, and the signal of the OAc group of the encapsulated **G** appeared at –1.93 ppm (Figure 6d and Figure S13d). However, the signal of **L3** was not observed, in contrast to **G**/**G**@(**2•1-Zn•L3•1-Zn•2**). The signal of the pyrrole-βH at 9.09 ppm was shifted downfield by 0.30 ppm relative to that of **G**/**G**@(**2•1-Zn•L3•1-Zn•2**) (δ = 8.79 ppm) (Figure 6d vs. 6c). The expansion spectra of Figures 6c and 6d are shown in Figures 7b and 7c, respectively. It is known that the signals of the pyrrole-βH and the OH group of the subunit-**3-Zn** and the signal of the OAc group of the encapsulated **G** for **G**@(**2•3-Zn**) appear at 9.34, 11.63, and –1.90 ppm, respectively, and those for **G**@(**2•3-Zn**)**•L2** appear at 9.42, 11.67, and –1.86 ppm, respectively.[6b] These results suggest that a 2:1:2:17 mixture of **3-Zn**, **L3**, **2**, and **G** was observed as an averaged form in an equilibrium mixture of **G**/**G**@(**2•3-Zn•L3•3-Zn•2**), **G**@(**2•3-Zn**)**•L3** + **G**@(**2•3-Zn**), and **G**@(**2•3-Zn**) + **L3**, due to fast exchanges of **L3** coordinated to the subunit-**3-Zn** (Figure 6d vs. 6c and Figure 7c vs. 7b), wherein relatively weaker ArOH···OH(Ar) hydrogen bonds between two **3-Zn** subunits are replaced by relatively stronger ArOH···Npy hydrogen bonds between **3-Zn** and **2** (Scheme 7B). In the 2D NOESY spectrum under the same conditions of Figure 6d, an exchange cross-peak was observed between H_2O signal and the signal at 11.59 ppm corresponding to the ArOH···Npy hydrogen bonds between the subunit-**3-Zn** and the subunit-**2**, but a signal corresponding to ArOH···OH(Ar) hydrogen bonds between two **3-Zn** subunits was not observed (Figure S14). These results indicate that **G**/**G**@(**2•1-Zn•L3•1-Zn•2**) is thermodynamically more stable than **G**/**G**@(**2•3-Zn•L3•3-Zn•2**). Thus, the assistance of ArOH···OH(Ar) hydrogen bonds between two **1-Zn** subunits plays an important role in the self-assembly of **G**/**G**@(**2•1-Zn•L3•1-Zn•2**).

Conclusion

We have demonstrated the quantitative self-assembly of a 1:2 mixture of Zn-*meso*-tetrakis(4-dodecyl-3,5-dihydroxyphenyl)porphyrin (**1-Zn**) and a bowl-shaped tetrakis(4-pyridylethynyl)cavitand (**2**) into the doubly cavitand-capped porphyrin capsule **2•1-Zn•2** in C_6D_6 via eight ArOH···Npy hydrogen bonds, but no Zn–Npy coordination bond between **1-Zn** and **2**. Capsule **2•1-Zn•2** with two cavities divided by the porphyrin ring encapsulated two molecules of 1-acetoxy-3,5-dimethoxybenzene (**G**) as a guest to form **G**/**G**@(**2•1-Zn•2**). Upon addition of 4-(4-methylphenyl)pyridine (**L2**) to **G**/**G**@(**2•1-Zn•2**), simultaneous encapsulation of **G** and **L2** in **2•1-Zn•2** preferentially occurred to form **G**/**L2**@(**2•1-Zn•2**). Under the conditions of [**2•1-Zn•2**] = 2 mM and [**G**] = [**L2**] = 17 mM in C_6D_6 at 298 K, the formation ratio of **G**/**L2**@(**2•1-Zn•2**) to **G**/**G**@(**2•1-Zn•2**) reached 91:9. By contrast, a 1:1:1 mixture of **1-Zn**, **L2**, and **2** in the presence of **G** self-assembled preferentially into the **G**-encapsulating half-capsule **G**@(**2•1-Zn**)**•L2** with coordination of **L2** at the outer side of **2•1-Zn**, together with **G**/**L2**@(**2•1-Zn•2**) and **G**/**G**@(**2•1-Zn•2**) as minor assemblies. When **L3** (DABCO) as a ditopic ligand was used in place of **L2**, a 2:1:2 mixture of **1-Zn**, **L3**, and **2** in the presence of **G** self-assembled preferentially into the **G**-encapsulating doubly cavitand-capped double-decker Zn-porphyrin capsule **G**/**G**@(**2•1-Zn•L3•1-Zn•2**) through coordination of **L3** between two **1-Zn** subunits and by the assistance of ArOH···OH(Ar) hydrogen bonds between two **1-Zn** subunits, together with **G**@(**2•1-Zn**) and **G**/**G**@(**2•1-Zn•2**) as minor assemblies. Under the conditions of a 2:1:2:17 mixture of **1-Zn** (2.0 mM), **L3**, **2**, and **G**, the formation ratio of **G**/**G**@(**2•1-Zn•L3•1-Zn•2**), **G**@(**2•1-Zn**), and **G**/**G**@(**2•1-Zn•2**) was found to be 1.00:0.61:0.18. Thus, selective formation of these cavitand–porphyrin capsules can be controlled by the stoichiometry of **1-Zn** and **2** as well as the character of N-ligands **L2** and **L3** in the presence of guest **G**.

A study on a self-assembled doubly cavitand-capped multi-decker metalloporphyrin capsule is underway in our laboratory.

Acknowledgements

This work was supported in part by JSPS KAKENHI Grant Number JP 17H03021 and Research Institute of Green Science and Technology Fund for Research Project Support (2020-20C02) at Shizuoka University.

Keywords: cavitands • host-guest systems • porphyrins • self-assembly • supramolecular chemistry

[1] a) A. Satake, Y. Kobuke, *Tetrahedron* **2005**, *61*, 13-41; b) I. Beletskaya, V. S. Tyurin, A. Y. Tsivadze, R. Guilard, C. Stern, *Chem. Rev.* **2009**, *109*, 1659-1713; c) N. Aratani, D. Kim, A. Osuka, *Acc. Chem. Res.* **2009**, *42*, 1922-1934; K. Gopalaiah, *Chem. Rev.* **2013**, *113*, 3248-3296; d) P. S. Bols, H. L. Anderson, *Acc. Chem. Res.* **2018**, *51*, 2083-2092; e) R. D. Mukhopadhyay, Y. Kim, J. Koo, K. Kim, *Acc. Chem. Res.* **2018**, *51*, 2730-2738.

[2] a) K. Harris, D. Fujita, M. Fujita, *Chem. Commun.* **2013**, *49*, 6703-6712; b) A. M. Castilla, W. J. Ramsay, J. R. Nitschke, *Acc. Chem. Res.* **2014**, *47*, 2063-2073; c) K. Kobayashi, M. Yamanaka, *Chem. Soc. Rev.* **2015**, *44*, 449-466; d) H. Sepehrpour, W. Fu, Y. Sun, P. J. Stang, *J. Am. Chem. Soc.* **2019**, *141*, 14005-14020; e) K. Wang, J. H. Jordan, X.-Y. Hu, L. Wang, *Angew. Chem. Int. Ed.* **2020**, *59*, 13712-13721; *Angew. Chem.* **2020**, *132*, 13816-13825.

[3] S. Durot, J. Taesch, V. Heitz, *Chem. Rev.* **2014**, *114*, 8542-8578, and references therein.

[4] For macrocyclic host-capped self-assembled porphyrin capsules, see a) R. Fiammengo, P. Timmerman, J. Huskens, K. Versluis, A. J. R. Heck, D. N. Reinhoudt, *Tetrahedron* **2002**, *58*, 757-764; b) H. Ohkawa, S. Arai, S. Takeoka, T. Shibue, H. Nishide, *Chem. Lett.* **2003**, *32*, 1052-1053; c) S. Arai, H. Ohkawa, S. Ishihara, T. Shibue, S. Takeoka, H. Nishide, *Bull. Chem. Soc. Jpn.* **2005**, *78*, 2007-2013; d) J. Nakazawa, M. Mizuki, Y. Shimazaki, F. Tani, Y. Naruta, *Org. Lett.* **2006**, *8*, 4275-4278; e) T.-H. Chiang, C.-Y. Tsou, Y.-H. Chang, C.-C. Lai, R. P. Cheng, S.-H. Chiu, *Org. Lett.* **2021**, *23*, 5787-5792.

[5] For covalently bound calixarene-capped porphyrin and calix[4]resorcinarene-cavitand-capped porphyrin, see: a) D. M. Rudkevich, W. Verboom, D. N. Reinhoudt, *J. Org. Chem.* **1995**, *60*, 6585-6587; b) Middel, O.; Verboom, W.; Reinhoudt, D. N. *J. Org. Chem*. **2001**, *66*, 3998-4005; c) J. Nakazawa, J. Hagiwara, Y. Shimazaki, F. Tani, Y. Naruta, *Bull. Chem. Soc. Jpn.* **2012**, *85*, 912-919.

[6] a) K. Kishimoto, M. Nakamura, K. Kobayashi, *Chem. Eur. J.* **2016**, *22*, 2629-2633; b) K. Nakabayashi, K. Kobayashi, *Chem. Lett.* **2017**, *46*, 1777-1780.

[7] a) K. Kobayashi, Y. Yamada, M. Yamanaka, Y. Sei, K. Yamaguchi, *J. Am. Chem. Soc.* **2004**, *126*, 13896-13897; b) M. Yamanaka, Y. Yamada, Y. Sei, K. Yamaguchi, K. Kobayashi, *J. Am. Chem. Soc.* **2006**, *128*, 1531-1539.

[8] It is known that the one-point hydrogen bond between *p*-methylphenol and *p*-methylpyridine is very weak: the association constant (K_a) = 31 M^{-1} in [D_8]toluene and K_a = 19 M^{-1} in $CDCl_3$ at 298 K. C. C. Robertson, J. S. Wright, E. J. Carrington, R. N. Perutz, C. A. Hunter, L. Brammer, *Chem. Sci.* **2017**, 8, 5392-5398.

[9] It is known that the K_a values of Zn-tetraphenylporphyrin (Zn-TPP) with 4-*tert*-butylpyridine (**L1**)[5a] or 4-phenylpyridine[5b] as an analog of **L2** are $K_a = 3.0 \times 10^3$ M^{-1} and $K_a = 1.4 \times 10^3$ M^{-1}, respectively, in $CDCl_3$ at 293 K.

[10] The K_a value of Zn-TPP with pyridine is $K_a = 3.3 \times 10^3$ M^{-1} in toluene at 298 K and the exchange between the coordinated and free pyridines is fast on the NMR time scale.[1a]

[11] K. Ichihara, H. Kawai, Y. Togari, E. Kikuta, H. Kitagawa, S. Tsuzuki, K. Yoza, M. Yamanaka, K. Kobayashi, *Chem. Eur. J.* **2013**, *19*, 3685-3692.

[12] a) P. N. Taylor, H. L. Anderson, *J. Am. Chem. Soc.* **1999**, *121*, 11538-11545; b) P. Ballester, A. Costa, A. M. Castilla, P. M. Deyà, A. Frontera, R. M. Gomila, C. A. Hunter, *Chem. Eur. J.* **2005**, *11*, 2196-2206; c) P. Ballester, A. I. Oliva, A. Costa, P. M. Deyà, A. Frontera, R. M. Gomila, C. A. Hunter, *J. Am. Chem. Soc.* **2006**, *128*, 5560-5569; d) J. K. Sprafke, B. Odell, T. D. W. Claridge, H. L. Anderson, *Angew. Chem. Int. Ed.* **2011**, *50*, 5572-5575; *Angew. Chem.* **2011**, *123*, 5687-5690; e) K. Stout, T. P. J. Peters, M. F. J. Mabesoone, F. L. L. Visschers, E. M. Meijer, J.-R. Klop, J. van den Berg, P. B. White, A. E. Rowan, R. J. M. Nolte, J. A. A. W. Elemans, *Eur. J. Org. Chem.* **2020**, 7087-7100.

[13] a) P. Thordarson, R. G. E. Coumans, J. A. A. W. Elemans, P. J. Thomassen, J. Visser, A. E. Rowan, R. J. M. Nolte, *Angew. Chem. Int. Ed.* **2004**, *43*, 4755-4759; *Angew. Chem.* **2004**, *116*, 4859-4863; b) S. Cantekin, A. J. Markvoort, J. A. A. W. Elemans, A. E. Rowan, R. J. M. Nolte, *J. Am. Chem. Soc.* **2015**, *137*, 3915-3923.

[14] For ArOH···OH(Ar) hydrogen-bonded networks of tetrakis- or bis(3,5-dihydroxyphenyl)porphyrins in the solid state, see: a) P. Bhyrappa, S. R. Wilson, K. S. Suslick, *J. Am. Chem. Soc.* **1997**, *119*, 8492-8502; b) K. Kobayashi, M. Koyanagi, K. Endo, H. Masuda, Y. Aoyama, *Chem. Eur. J.* **1998**, *4*, 417-424.

Entry for the Table of Contents

Insert graphic for Table of Contents here.

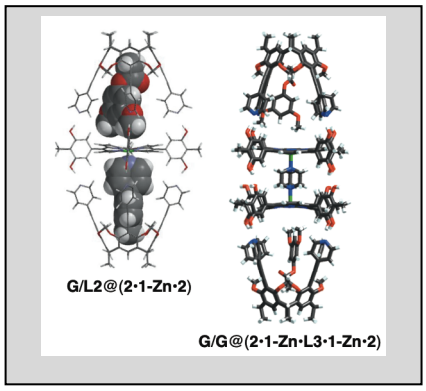

Selective formation of cavitand-capped Zn-porphyrin-sandwich capsules such as **G**/**L2**@(**2**•**1-Zn**•**2**) and **G**/**G**@(**2**•**1-Zn**•**L3**•**1-Zn**•**2**) can be controlled by the stoichiometry of porphyrin **1-Zn** and cavitand **2** as well as the character of N-ligands **L2** and **L3** in the presence of guest **G**.